Developmental Defects in a *Caenorhabditis elegans* Model for Type III Galactosemia

Ana M. Brokate-Llanos,* José M. Monje,* Piedad del Socorro Murdoch,† and Manuel J. Muñoz*,[1]

*Centro Andaluz de Biología del Desarrollo, Consejo Superior de Investigaciones Científicas–Universidad Pablo de Olavide–Junta de Andalucía, 41013 Seville, Spain, and †Departamento de Bioquímica y Biología Molecular, Facultad de Biología, Universidad de Sevilla, 41012 Seville, Spain

ABSTRACT Type III galactosemia is a metabolic disorder caused by reduced activity of UDP-galactose-4-epimerase, which participates in galactose metabolism and the generation of various UDP-sugar species. We characterized *gale-1* in *Caenorhabditis elegans* and found that a complete loss-of-function mutation is lethal, as has been hypothesized for humans, whereas a nonlethal partial loss-of-function allele causes a variety of developmental abnormalities, likely resulting from the impairment of the glycosylation process. We also observed that *gale-1* mutants are hypersensitive to galactose as well as to infections. Interestingly, we found interactions between *gale-1* and the unfolded protein response.

GALACTOSE is universally metabolized by three conserved enzymes that constitute the Leloir pathway (Figure 1) (Holden *et al.* 2003). UDP-galactose-4-epimerase (GALE) participates in the third step of the galactose metabolism pathway, catalyzing the interconversion of UDP-galactose (UDP-gal) and UDP-glucose (UDP-glc) and in some species, including humans, also the interconversion of UDP-*N*-acetylgalactosamine (UDP-galNAc) and UDP-*N*-acetylglucosamine (UDP-glcNAc) (Figure 1) (Maley and Maley 1959; Piller *et al.* 1983; Kingsley *et al.* 1986; Wohlers *et al.* 1999). Thus, GALE is essential not only to use galactose as an energy source but also to produce the different species of UDP sugars required for the glycosylation of proteins and lipids.

In humans, mutations in GALE result in an autosomal recessive disorder known as type III galactosemia (OMIM #230350) (Fridovich-Keil 2006; Timson 2006), a rare disease characterized by the inability to metabolize galactose with symptoms that can include early onset cataracts, liver damage, deafness, and mental retardation (Walter *et al.* 1999). These symptoms are thought to occur as a result of the accumulation of intermediary galactose metabolites and the reduction of UDP-sugar species, which are needed for glycosylation. Other types of galactosemia are treated with a galactose-free diet. However, because of the dual role of GALE, patients with type III galactosemia are recommended to follow a galactose-restricted diet to avoid UDP-gal deficiency. This diet only partially alleviates the severe symptoms of galactosemia type III (Walter *et al.* 1999), and it has been proposed that patients receive UDP-galNAc as an additional treatment (Kingsley *et al.* 1986).

Traditional model systems to study type III galactosemia include yeast, which does not exhibit the interconversion of UDP-N acetylgalactosamine and UDP-N acetylglucosamine (Schulz *et al.* 2004), and cell lines, such as human fibroblasts and the ldlD cell line derived from Chinese hamster ovaries. The latter exhibits a complete loss of GALE activity, resulting in the abnormal processing of both N- and O-linked glycoproteins (Kingsley *et al.* 1986; Krieger *et al.* 1989; Slepak *et al.* 2007). Recently, the first multicellular model for this disease was generated in *Drosophila*, in which the deletion of GALE caused a lethal phenotype (Sanders *et al.* 2010). In the present study, we propose the use of *Caenorhabditis elegans* as a model to better understand the role of GALE in development and the consequences of its malfunctioning in multicellular organisms.

The free-living nematode *C. elegans* has been very useful for studies of development, disease, and other biological processes, including glycosylation (Culetto and Sattelle 2000; Kuwabara and O'Neil 2001; Berninsone and Hirschberg 2002; Berninsone 2006). Different mutations affecting enzymes

doi: 10.1534/genetics.114.170084
Manuscript received August 21, 2014; accepted for publication October 1, 2014; published Early Online October 8, 2014.
Supporting information is available online at http://www.genetics.org/lookup/suppl/doi:10.1534/genetics.114.170084/-/DC1.
[1]Corresponding author: Centro Andaluz de Biología del Desarrollo, CSIC/Universidad Pablo de Olavide, Carretera Utrera Km. 1, 41013 Seville, Spain. E-mail: mmunrui@upo.es

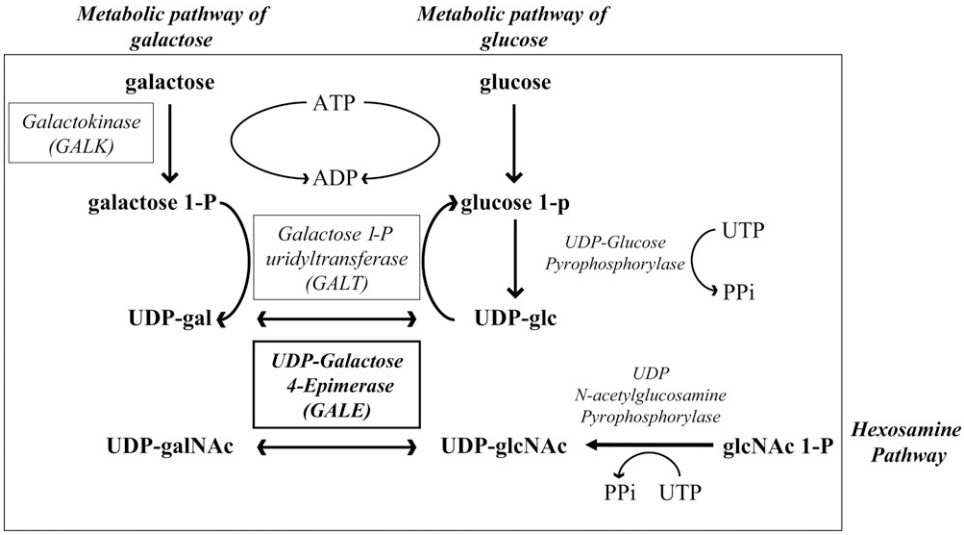

Figure 1 The role of GALE in the biosynthesis of different UDP sugars. The enzymes in the Leloir pathway are boxed. GALE participates in the third step of the Leloir pathway and in the production of UDP-galNAc and UDP-glcNAc. Other metabolic pathways that participate in the production of UDP-glc and UDP-glcNAc are also represented.

involved in proteoglycan synthesis, N-glycosylation, O-glycosylation, and chitin and glycolipid synthesis have been isolated in this organism. Genetic and biochemical studies have demonstrated that most of the genes involved in glycosylation are conserved in humans (Schachter 2004; Berninsone 2006). Interestingly, most mutations affecting the glycosylation process show developmental defects. For example, most of the mutants defective in vulval epithelial invagination, the *sqv* mutant class, result from genes involved in the biosynthesis of the glycosaminoglycan chondroitin (Herman *et al.* 1999; Berninsone 2006), and mutations that affect N-glycosylation lead to the development of misshapen gonads. One of the genes involved in gonad development is MIG-17, a member of the ADAM (a disintegrin and metalloprotease) family. MIG-17 is a glycoprotein that is secreted by muscle cells and diffuses to the basement membrane of the gonad, where its function is required (Nishiwaki *et al.* 2000, 2004). Mutations that affect the MIG-17 glycosylation state prevent MIG-17 localization to the basement membrane and, as a consequence, exhibit a gonad migration defect similar to that of *mig-17* mutants (Nishiwaki *et al.* 2000, 2004; Kubota *et al.* 2006). The analysis of mutants in which gonad migration is affected has enabled the identification of many different elements involved in the glycosylation process, indicating that *C. elegans* is an appropriate model for studying the mechanisms of glycosylation during development (Kubota and Nishiwaki 2006).

The process of protein glycosylation begins in the endoplasmic reticulum (ER), which is also responsible for protein folding, trafficking, quality control, degradation, and the coordinated response to the accumulation of unfolded proteins. Three proteins, conserved in all metazoans, are involved in sensing the stress caused by the accumulation of unfolded proteins (Bernales *et al.* 2006; Malhotra and Kaufman 2007): the protein kinase PERK (protein kinase RNA-like endoplasmatic reticulum kinase); the transcription factor ATF-6 (activating transcription factor 6); and XBP-1 (Xbox binding protein), a transcription factor that is activated after cleavage of the *xbp-1* messenger RNA by IRE-1 (inositol-requiring enzyme 1; endonuclease resident in the ER). These sensors activate the unfolded protein response (UPR) pathway, initiating a complex response that involves the degradation of proteins, shuts off general translation, and enhances the expression of chaperones, such as the heat-shock proteins *hsp-4* and *hsp-3* in *C. elegans* (Lee 1992; Schroder and Kaufman 2005a,b; Shen *et al.* 2005).

Here, we characterize two different alleles of *gale-1*, the single homolog of the GALE gene in *C. elegans* that has 57% identity with the human GALE. The knockout allele is lethal, arresting development in the L2 larval stage, whereas a reduction-of-function allele is viable, although it exhibits severe developmental abnormalities consistent with impairment in protein glycosylation. This hypomorphic mutant is similar to the condition found in type III galactosemia patients and enables further characterization of *gale-1* impairment. As described in humans and in model systems, this mutant strain is hypersensitive to a galactose-rich diet. Interestingly, it is also hypersensitive to human bacterial pathogens. We have also observed ER stress in the *gale-1* reduction-of-function allele.

Materials and Methods

Strains and general methods

For the *C. elegans* strains, N2 and mutants were cultivated under standard conditions (Brenner 1974). The strains used are as follows: N2, GM107 [*gale-1(pv18)*], FX03267 *gale-1(tm3267)*, MT7562 *sqv-7(n2839)*, WT; Ex(mig-17::GFP), *mig-23(k180)*; Ex(mig-17::GFP), GM238 *gale-1(pv18)*; Ex[mig-17::GFP], GM328 *sqv-7(n2839)*; Ex[mig-17::GFP], BC11076 C47B2.6::GFP, SJ4005 *zcls4(hsp-4::gfp)*, GM266 *gale-1(pv18)*; *zcls4(hsp-4::gfp)*, GM308 *atf-6(ok551)*; *fer-15(b26)*, and GM 268 *gale-1(pv18)*; *pvIs1*(*C47B2.6 pgk10*).

Bacterial strains included *Escherichia coli* OP50 and HT115, *Enterococcus faecalis*, *Staphylococcus aureus*, and *Pseudomonas aeruginosa*.

gale-1(pv18) mapping and identification

Genetic mapping using visible markers and nucleotide polymorphisms (Wicks *et al.* 2001) located the mutation in an interval of ~60 kb on the right arm of chromosome I. Transgenic lines carrying cosmids mapped to this area revealed that the cosmid C47B2 complemented the mutant *gale-1(pv18)* phenotype. The five genes located in this cosmid were sequenced in the wild-type and in the *pv18* mutant strain, revealing a mutation in the *gale-1* gene, corresponding to the gene C47B2.6. Complementation of the temperature-sensitive lethal phenotype of *gale-1(pv18)* with a construct containing only the wild-type *gale-1* gene driven by its own promoter demonstrated that *pv18* is an allele of *gale-1* UDP-galactose-4-epimerase.

This construct was generated by amplifying the *gale-1* gene using the oligos 5′ TCTGACACCACGTGAAAACC 3′ and 5′ AGGTCCTACCGATGATGACG 3′ and by introducing the resulting PCR fragment into the pGEM-T Easy vector (Invitrogen). To generate the transgenic lines, we used the particle gun designed by Ralf Schnabel (http://www.ifg.tu-bs.de/Schnabel/) following the protocol described by Wilm *et al.* (1999). Transgenic lines were selected by screening for expression from the cotransfected plasmid pGK10 (*sca-1*::*GFP*) (Zwaal *et al.* 2001) using a Leica Fluo III stereoscope. In addition to the lethal temperature-sensitive phenotype, this construction fully rescues hypersensitivity to galactose, vulval, and gonad morphogenesis and hypersensibility to infection and rescues partially the synergistic lethal effect on *xbp-1* RNA interference (RNAi).

Bacterial pathogen assay

Wild-type and *gale-1(pv18)* mutant worms (10 L4 per plate) were grown in the presence of pathogenic bacteria as the sole food source, and the numbers of survivors were counted every 2 days. *E. faecalis* strain OG1RF was grown in brain heart infusion with 40 μg/ml of gentamycin. *S. aureus* strain NTCT8325 was grown in Trypticase Soy Broth with 10 μg/ml of nalidixic acid.

Treatment with sugars

Eggs were incubated on NGM plates containing 0, 0.5, 1, 2, or 3% D-galactose (Sigma, G0625), D-glucose (Panreac 131341.0914), D-mannose (Fluka 63580), or L-glucose (G5500). Animals were scored after 4 days at 20°. Experiments with UV-killed bacteria were performed as described by Gems and Riddle (2000).

RNAi assays

RNAi feeding was performed as described in Kamath *et al.* (2003). L4 hermaphrodites were transferred to empty plasmid control pL4440 or to the appropriate RNAi plates at 20°, and the subsequent generation was analyzed.

Microscopy

L4 worms were mounted in M9 buffer between a coverslip and a 2% agarose pad. Images of the whole worm of SJ4005 and GM266 strains were captured using a Zeiss Axio Imager M2 microscope with N-Achroplan 10× and Plan Apochromat 10× objectives and a GFP-FITC-A488 filter. For MIG-17::GFP, we used an EC-Plan Neofluar ×40 objective. All pictures were acquired under the same conditions and with identical exposure time. For eggs, gonads, and vulva, we used this objective with Nomarski optics.

For coelomocytes, transmitted light and epifluorescence were recorded with a Nikon-A1R confocal microscope through a 60×/1.4 objective, captured using integral Nikon software.

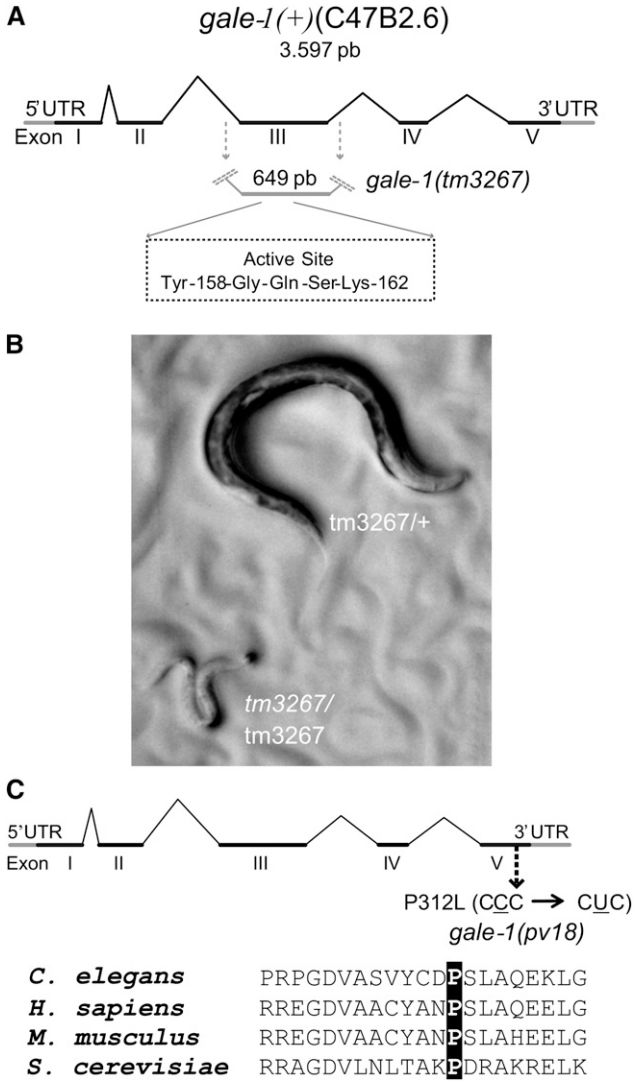

Figure 2 Locations of the *gale-1(tm3267)* and *gale-1(pv18)* mutations. (A) The *gale-1(tm267)* allele lacks a central region of the protein that contains the active site (YXXXK). (B) *gale-1(tm267)* homozygous mutants arrest during development at L2 stage with reduced movement and pale body color. The genotypes of these animals were confirmed by PCR. (C) *gale-1(pv18)* is a missense mutation that generates the substitution of a proline for a leucine residue in a conserved region.

HPLC

Whole extracts from 1000 young wild-type and *gale-1(pv18)* hermaphrodites were analyzed. Animals were collected in

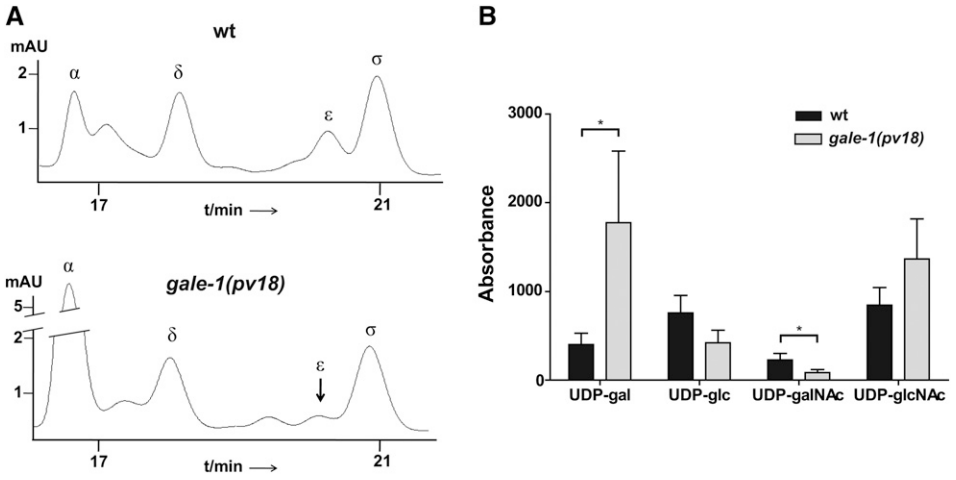

Figure 3 RP-HPLC profile of the UDP-sugars synthesized by *gale-1* in the *gale-1(pv18)* mutant. (A, Top) A representative profile from an extract of 1000 wild-type young adult worms. (Bottom) A representative profile from an extract of 1000 *gale-1(pv18)* young adult worms grown under the same conditions. α, UDP-gal; δ, UDP-glc; ε, UDP-galNAc; σ, UDP-glcNAc. (B) Mean and standard deviation of the absorbance area of the four sugars in three different repetitions for each strain. Two tailed *t*-test shows that only the differences in the UDP-gal and UDP-GalNAc levels are statistically significant. $*P < 0.05$.

M9 buffer, incubated for 30 min at room temperature, washed three times in 3 ml of H_2O, resuspended in 50 μl H_2O, freeze-thawed three times on methanol/dry ice, and stored at −80°. For cell disruption, samples were thawed rapidly, and 500 μl of glass beads (0.2–1.5 g glass beads/ml, 0.1 mm diameter; Cole Parmer) was added at 4°. Bead-vortexing was performed at 4° on a Hybaid Ribolyser Mixer at 3000 × *g* for 1 min. After disruption, samples were centrifuged at top speed at 4° for 15 min. The supernatant was filtered and injected onto an reversed phase (RP) HPLC column (Supelcosil LC-18-T HPLC column, 5-μm particle size, length × i.d. of 25 cm × 4.6 mm). Detection was conducted by ultraviolet absorption at 262 nm (absorbance detector, Waters). The mobile phase was conducted with 150 mM KH_2PO_4 containing 2 mM tetrabutylammonium phosphate monobasic (Aldrich), pH 6.75, at a flow of 0.5 ml/min. Before and after each set of runs, standards of all four UDP sugars were injected and quantified. The UDP sugars of interest (UDP-gal, UDP-glc, UDP-galNAc, and UDP-glcNAc) demonstrated baseline separation.

Results

gale-1 mutations

We characterized two different *gale-1* alleles: *gale-1(tm3267)* and *gale-1(pv18)*. In *gale-1(tm3267)*, 649 bp encompassing the third exon in addition to the flanking intronic sequences have been replaced by an insertion of 6 bp, removing the active site of the GALE-1 protein (Thoden and Holden 1998; Thoden *et al.* 2001), which indicates that *gale-1(tm3267)* is a knockout allele (Figure 2A). Homozygous animals carrying this allele arrested in the L2 larval stage and exhibited a lethargic phenotype and pale body color (Figure 2B). This lethal phenotype complicated further characterization and is distinct from the condition of humans with type III galactosemia, who exhibit a reduction of GALE activity that generates a variety of disorders; no patients have been found to completely lack GALE function (Timson 2006).

Using the selection protocol for thermotolerant L1 larvae described in Munoz and Riddle (2003), we isolated the viable *gale-1(pv18)* mutant, which carries a leucine substitution for a conserved proline at position 312, which is close to the N-acetyl group interaction site (Figure 2C) (Thoden *et al.* 2001; Thoden *et al.* 2002) (see *Materials and Methods* for gene identification). Phenotypes of the maternal-effect mutant *gale-1(pv18)* described below and the lethal phenotype of *gale-1(tm3267)* were rescued with a transgene carrying the *gale-1* wild-type allele driven by 1.2 kb upstream of the ORF, indicating that they are caused by the mutations in the *gale-1* gene.

gale-1(pv18) is impaired in UDP-sugar levels

Using RP-HPLC, we compared the profile of the UDP-sugars synthesized by GALE-1 in the wild-type and *gale-1(pv18)* strains and found that mutant worms fed the standard *E. coli* strain OP50 accumulate UDP-gal and exhibit diminished levels of UDP-galNAc (Figure 3, A and B), as expected in response to a general reduction of the function of the *gale-1* gene. Changes in UDP-glc and UDP-glcNAc are not significant. Interestingly, increased UDP-gal levels have been also observed in human patients (Walter *et al.* 1999) as in the yeast model for galactosemia type III (Quimby *et al.* 1997; Ross *et al.* 2004; Wasilenko *et al.* 2005; Chhay *et al.* 2008).

gale-1(pv18) confers hypersensitivity to galactose

One of the symptoms of galactosemia is intolerance to a galactose-rich diet, which has been attributed to the accumulation of toxic galactose metabolism intermediates (Walter *et al.* 1999; Ross *et al.* 2004; Sanders *et al.* 2010; McCorvie *et al.* 2011). We observed that *gale-1(pv18)* worms cultivated in a high concentration of galactose develop slowly, indicating a hypersensitivity to galactose, whereas wild-type worms or *gale-1(pv18)* carrying a construction with *gale-1(+)* are not affected (Figure 4A). Interestingly, a percentage of animals cultivated in galactose were arrested at the L1 stage of development in a dosage-dependent manner, which was not observed in the wild-type strain. These animals showed a swollen and dark body (Figure 4, B and C). To test if this effect is specific to galactose, we also assayed different sugars

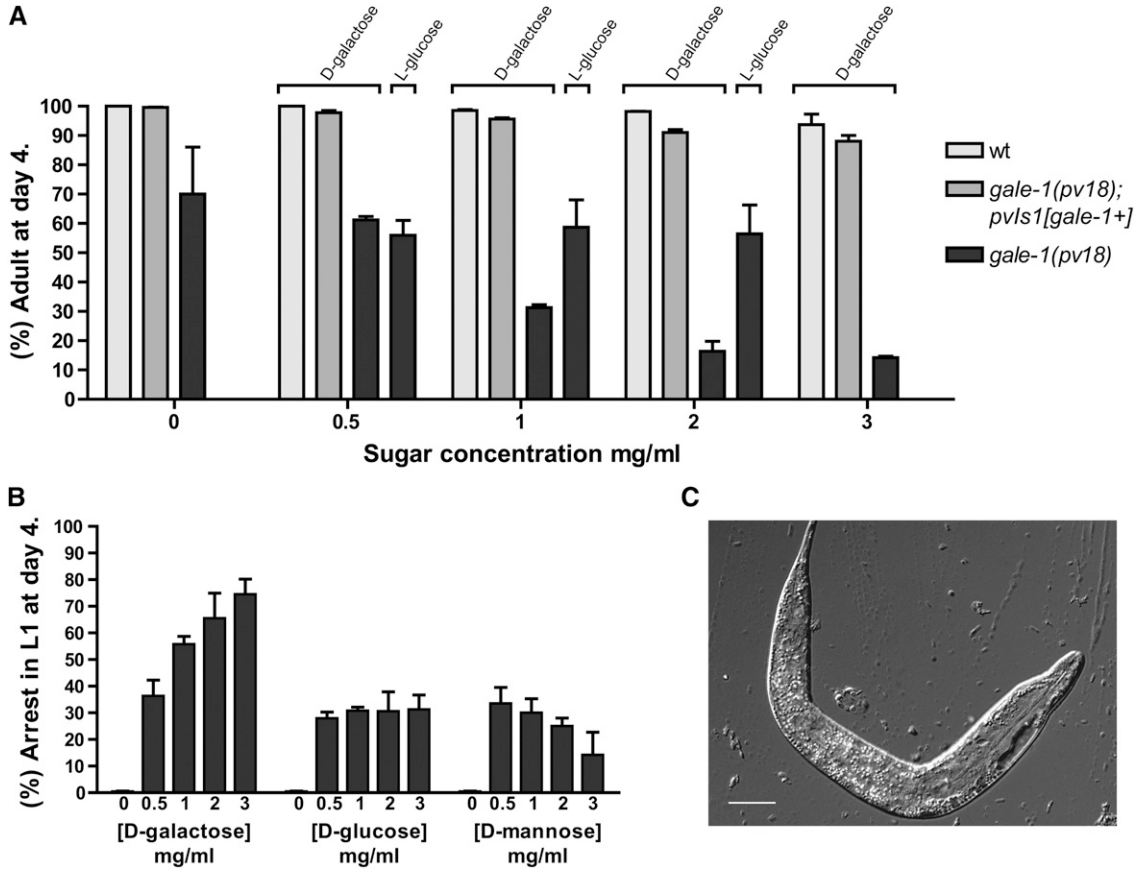

Figure 4 Galactose sensitivity of *gale-1(pv18)*. (A) The percentage (%) of animals reaching adulthood after 4 days of incubation at different concentrations of D-galactose. Dramatically fewer *gale-1(pv18)* animals reached adulthood at the highest concentration of D-galactose, whereas wild-type or *gale-1(pv18)* transgenic with *gale-1(+)* animals were hardly affected. The nonmetabolizable sugar L-glucose does not affect development of *gale-1 (pv18)* at any concentration assayed. There are no significant differences between wild type at 0 and any galactose concentration. There are significant differences between *gale-1(pv18)* at 0 and 1–3 mg/ml of galactose. $P < 0.1$. (B) The percentage (%) of animals arrested in L1 at different concentrations of galactose, glucose, or mannose. Treatment with 0.5 mg/ml of any of the sugars generates a percentage of arrested animals. This percentage does not increase in higher concentrations of glucose or mannose ($P > 0.1$). At higher concentrations of galactose, the percentage of arrested animals increases ($P < 0.05$ for 0.5 mg/ml *vs.* any other concentration). (C) A representative L1-arrested animal in the presence of galactose. Bar, 15 μm. Data are from two different experiments with $n \geq 200$ in each.

in UV-killed bacteria to avoid interference with the bacterial metabolism, and, surprisingly, we found that treatment with glucose or mannose also generates a small percentage of L1 arrest. Interestingly, the percentage of arrested animals does not increase with the concentration of the sugar as happens with galactose (Figure 4B), indicating that galactose or metabolites derived from galactose have a more prominent effect on the L1 arrest phenotype.

gale-1(pv18) affects organ morphogenesis

gale-1(pv18), but not *gale-1(pv18)* rescued with *gale-1(+)*, worms exhibit multiple developmental defects. The animals develop more slowly at 16° and 20° than their wild-type counterparts (Supporting Information, Table S1), and their gonads are misshapen as a result of a migration defect (Figure 5, A and B). This last phenotype resembles those of mutants affected by alterations in the N-glycosylation process, such as *mig-17*, *mig-23*, and *cogc-1–8* (Nishiwaki *et al.* 2004; Kubota *et al.* 2006). As with the gonads in those mutants, we observed that the posterior gonad in *gale-1(pv18)* mutants is more prone to this defect (Figure 5C).

gale-1(pv18) worms also showed a small vulval lumen with a reduction of >50% in size at the L4 stage (Figure 5, D and E, and Figure S1). This phenotype is similar to that of the squashed-vulva mutant class "*sqv*," which primarily represents mutants in which the synthesis of the proteoglycan chondroitin is affected (Berninsone and Hirschberg 2002; Bulik and Robbins 2002; Hwang *et al.* 2003; Suzuki *et al.* 2006). Chondroitin is formed by repeated units of galNAc and glucuronic acid; therefore, the reduction of UDP-galNAc found in the *gale-1(pv18)* mutant is consistent with the impairment in the synthesis of this proteoglycan.

In addition, when *gale-1(pv18)* worms are reared at 25°, most embryos die before hatching and survivors arrest as L1 larvae. A closer inspection of the embryonic development showed frequent cell–cell adhesion defects, which caused embryos to disintegrate at an advanced stage of development. Additionally, some embryos failed to hatch even when

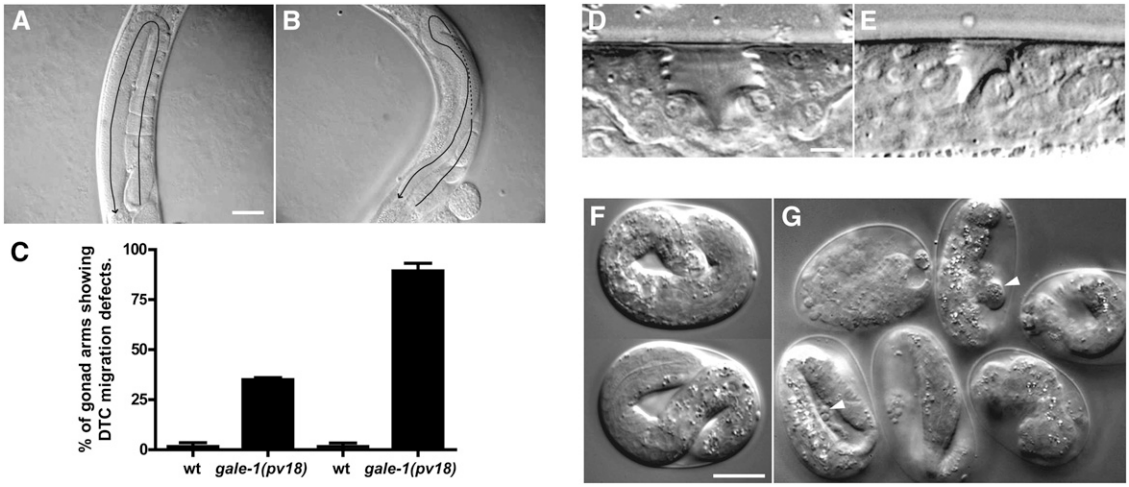

Figure 5 Developmental defect phenotypes of *gale-1(pv18)*. (A) Wild-type gonad, which exhibits a U-shape. (B) *gale-1(pv18)* gonad. In this mutant, the gonads exhibit an irregular shape and are not symmetrical as indicated by the arrow. (C) Percentage of abnormal gonads in wild-type (N2) and *gale-1* mutant. $n > 20$. $P < 0.05$. Animals were grown at 20°. (D) Wild-type vulva at the L4 stage. (E) Vulva of an L4 *gale-1(pv18)* animal. Note the reduced size (see also Figure S1). Animals were grown at 20°. (F) Wild-type embryos incubated at 25°. (G) *gale-1(pv18)* embryos incubated at 25°. Note the bubbles of embryonic material and vacuoles in the mutant indicated by arrowheads (see also File S1). Bars, 40 μm (A and B); 2.5 μm (D and E); and 20 μm (F and G).

they successfully completed morphogenesis (Figure 5, F and G, and File S1). The phenotypes described here indicate that the reduction of *gale-1* activity affects multiple aspects of development, likely as a result of a general defect in the glycosylation process.

To investigate the expression pattern of *gale-1*, we used the BC11076 strain, in which expression of GFP is driven by 2927 bp upstream of the ATG of *gale-1*. Previous reports indicate that *gale-1* is expressed mainly in the gonads, vulva, intestine, and nervous system in L4/adult-stage worms (WormBase: http://www.wormbase.org). We observed that *gale-1* is also expressed in muscle tissue. Especially high and broad *gale-1* expression was detected in embryos and in the L1 stage (Figure S2).

MIG-17 is mislocalized in the gale-1(pv18) mutant

To identify a possible mechanism for the gonad migration defects of *gale-1(pv18)*, we investigated the location of the metalloprotease MIG-17. To carry out its normal functions, N-glycosylated MIG-17 is secreted by muscle cells and localizes to the basement membrane of the gonad (Nishiwaki *et al.* 2004). Mutations in *mig-17* or in genes involved in MIG-17 glycosylation cause gonad migration defects similar to that described in the *gale-1(pv18)* mutant. We observed that MIG-17 localization to the gonad basement membrane is reduced in the *gale-1(pv18)* mutant (Figure 6, A and B), similarly to the *mig-23* mutant, which affects MIG-17 glycosylation (Figure 6D), and to mutations at MIG-17 glycosylation sites (Nishiwaki *et al.* 2004). This suggests that the impairment of MIG-17 glycosylation may be responsible for the gonad-migration phenotype observed in the *gale-1(pv18)* mutant.

sqv-7 encodes a protein that transports UDP-glucuronic acid, UDP-gal, and UDP-galNAc to the Golgi apparatus. The *sqv-7(n2839)* mutant exhibited both an *sqv* phenotype (Herman *et al.* 1999; Berninsone *et al.* 2001; Bulik and Robbins 2002; Hwang and Horvitz 2002) and, as we observed, a gonad migration defect similar to that of the *gale-1(pv18)* mutant (Figure S3). Interestingly, we found that MIG-17 is also mislocalized in an *sqv-7* mutant background (Figure 6C), suggesting that a decrease of UDP-sugar in the cytosol as a result of the *gale-1* mutation or in the Golgi as a result of impairment of SQV-7 activity generates improper glycosylation, incorrect localization, and the malfunctioning of MIG-17. Because UDP-galNAc is affected in both *gale-1* and *sqv-7* mutants, these data highlight UDP-galNAc as an important molecule in the *sqv* and *mig* phenotypes.

The phenotype of MIG-17 mislocalization could be due either to a defect in the secretion from the muscle cells or to the loss of affinity to the basal membrane of the gonad. To discriminate between these possibilities, we have studied the accumulation of MIG-17, labeled with GFP, in the coelomocyte cells. Those cells endocytose the pseudocoelom fluid and are useful to test if proteins are secreted from other cell types (Kubota *et al.* 2006). We have observed the presence of MIG-17-GFP in coelomocytes of *gale-1(pv18)* and *sqv-7(n2839)* mutants (Figure 7), indicating that MIG-17 is secreted from the muscle cells in both genetic backgrounds.

gale-1(pv18) activates the unfolded protein response pathway

Because the N-glycosylation process begins in the ER, we hypothesized that the altered UDP-sugar levels observed in the *gale-1(pv18)* mutant may affect the activity of this organelle and may activate the unfolded protein response pathway. One of the genes involved in this pathway is *xbp-1*, which produces an inactive transcript that is activated by the *ire-1*

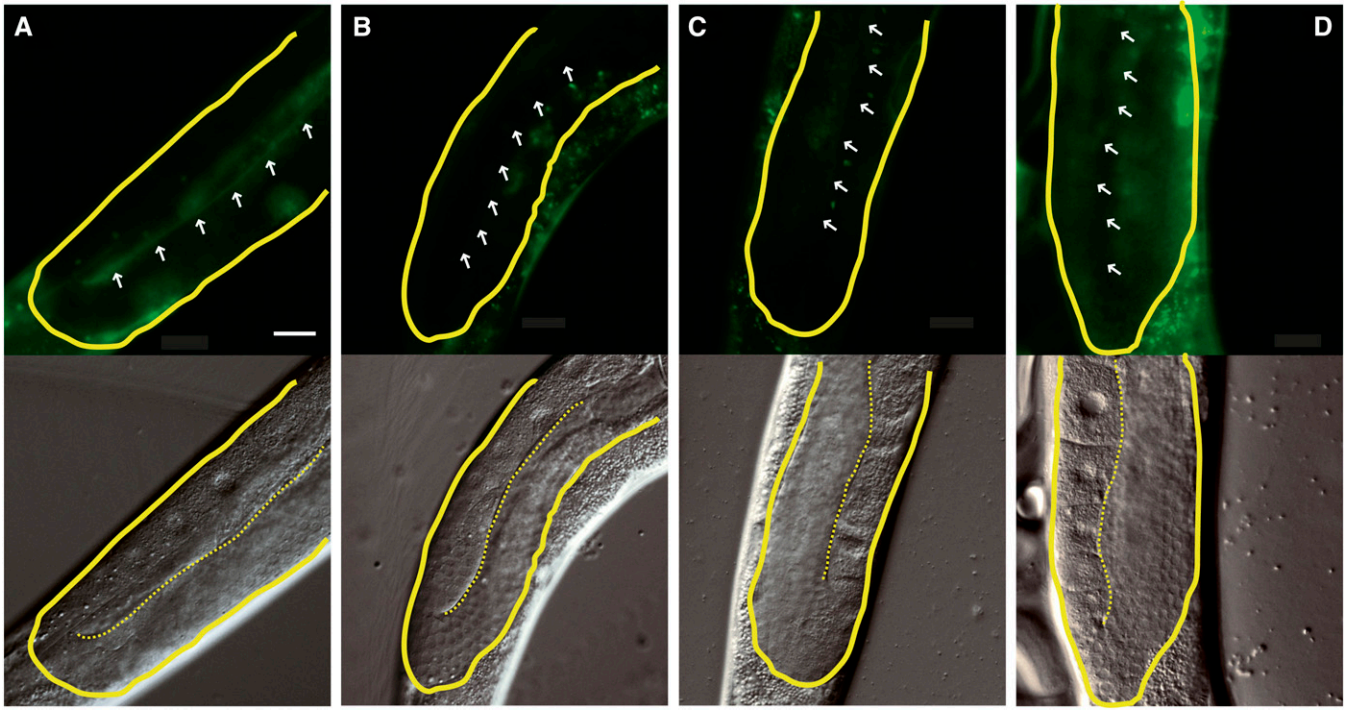

Figure 6 MIG-17 location is altered in *gale-1* and *sqv-7* mutant backgrounds. (Top) GFP fluorescence. (Bottom) Nomarski. White arrows indicate the location of the basement membrane. (A) MIG-17::GFP is located in the basement membrane of the gonad in a wild-type background; 32 ± 10.6% of increase of fluorescence level in the basement membrane relative to the central region of the gonad. $n = 8$. (B) In a *gale-1(pv18)* mutant background, the location of MIG-17::GFP in the basement membrane is reduced relative to wild-type background; 10.2 ± 3.9% increase of fluorescence level in the basement membrane relative to the central region of the gonad. $n = 8$. The differences with the wild-type background are significant; $P < 0.001$.Two tailed *t*-tests were used for comparison. (C) Similarly, in an *sqv-7(n2839)* background, MIG-17::GFP is also mislocalized. (D) *mig-23(k180)*, in which MIG-17::GFP has been reported to be mislocalized, was used as control. Bar, 20 μm.

endonuclease upon ER stress (Tirasophon *et al.* 1998; Wang *et al.* 1998). The transcription factor XBP-1 promotes the expression of numerous genes involved in the stress pathway, among them *hsp-4* (Calfon *et al.* 2002; Shen *et al.* 2005). We therefore tested the expression of *hsp-4*, and, as shown in Figure 8, A and B, the expression was ~2.5 times higher in *gale-1(pv18)* than in the wild type (Figure S4). A high level of *hsp-4* expression is also observed in a *atf-6(ok551)* mutant background (Figure S5). The reduction of XBP-1 or IRE-1 activity by RNAi completely suppresses *hsp-4* expression in both mutants (Figure 8, C and D, Figure S5, and data not shown). These results suggest that the expression of *hsp-4* in *atf-6(ok551)* and in *gale-1(pv18)* is caused by the activation of *xbp-1*.

xbp-1 participates together with another stress sensor, *atf-6*, in *C. elegans* development. Reduction of either of those genes independently does not affect development, but animals arrest in the L2 stage when both are simultaneously eliminated (Shen *et al.* 2005). We observed that *gale-1(pv18)* can develop to adulthood under *atf-6* RNAi treatment but arrest in the L2 stage under reduction of *xbp-1* activity by RNAi, similarly to *xbp-1* RNAi treatment of *atf-6* mutants (Figure 8E). This result suggests that *gale-1* and *atf-6* are involved in the same genetic pathway to affect development. Heteroallelic *tm3267/pv18* animals also arrest development when subjected to *xbp-1* RNAi (data not shown). *tm3267*; *xbp-1*(RNAi) animals are fully rescued by the *gale-1*+ transgene (data not shown) while *pv18*; *xbp-1*(RNAi) animals are not fully rescued to viability by this transgene; these animals, instead of arresting at the L2 stage as their not-transgenic siblings do, continue development to L4, but they do not reach adulthood. This result suggests a semidominant effect of *pv18* for this phenotype.

The expression of *hsp-4* and the arrest in development with the *xbp-1* RNAi treatment in *gale-1(pv18)* suggest that the endoplasmic reticulum is compromised in animals lacking normal GALE-1 activity.

gale-1(pv18) is hypersensitive to infection

Patients affected with type I galactosemia have been described as suffering an increased risk of infections (Levy *et al.* 1977; Litchfield and Wells 1978; Waggoner *et al.* 1990; Rathi and Rathi 2011). *C. elegans* is a widely used model to understand host–pathogen interaction, and many human bacterial pathogen have been described to affect this nematode (Sifri *et al.* 2005).

We tested the survival of *gale-1(pv18)* mutants grown in the presence of different species of human pathogenic bacteria that have been previously shown to infect *C. elegans* (Garsin *et al.* 2003). We observed that *gale-1(pv18)* animals incubated with *E. faecalis* or *S. aureus* (Figure 9) exhibited lower survival than wild-type worms but not when complemented with the transgene containing *gale-1(+)* (Figure S6), indicating that

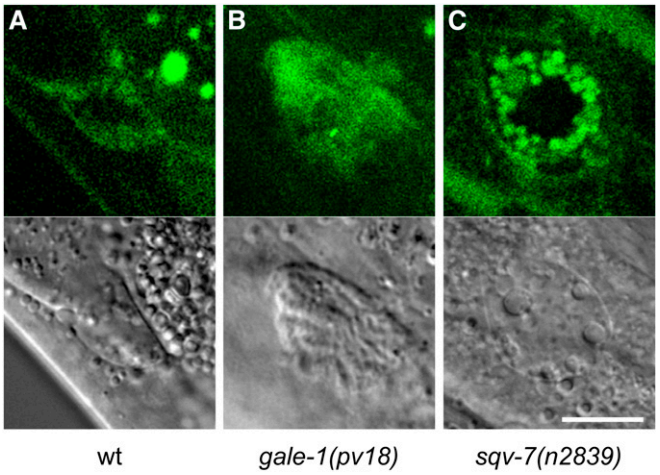

Figure 7 Uptake of MIG-17::GFP by coelomocytes. (Top) GFP fluorescence. (Bottom) Nomarski of the same coleomocytes. (A) MIG-17::GFP located in the coleomocytes in a wild-type background, (B) in a *gale-1 (pv18)* background, and (C) in a *sqv-7(n2839)* mutant background.

they are hypersensitive to infection. This result, if conserved in humans, may have medical implications for the management of patients with type III galactosemia.

Discussion

In this study, we have reported the characterization of two mutations in the *C. elegans* GALE ortholog, a knockout allele, and a reduction-of-function allele. We found that the loss of function of *gale-1* in *C. elegans* is lethal. The same lethal effect has also been shown in *Drosophila* and has been hypothesized for humans (Kalckar 1965; Sanders *et al.* 2010). This condition complicates phenotypic analysis and is dissimilar to the condition found in type III galactosemia in humans, in which patients exhibit a reduction of the GALE activity but never a complete lack of activity. We studied the reduction-of-function allele *gale-1(pv18)* in detail because this allele enables physiologic and genetic studies. We observed that the changes in the UDP-sugar profile found in *gale-1(pv18)* are consistent with a reduction of activity of GALE. The increased level of UDP-gal can be explained by the inability to metabolize dietary galactose, and the strong reduction of UDP-galNAc levels can be attributed to the fact that GALE is the primary enzyme responsible for UDP-galNAc biosynthesis. In contrast, UDP-glc and UDP-glcNAc are synthesized also by GALE-independent pathways (Figure 1), which may explain why the changes observed in the levels of these sugars are not statistically significant (Schulz *et al.* 2005; Johnston *et al.* 2006). These data, together with the recessive nature of *gale-1(pv18)*, strongly suggest that this is a viable reduction-of-function allele similar to the situation described in patients with type III galactosemia (Timson 2006). While all GALE homologs are able to metabolize UDP-gal and UDP-glc, not all the species are able to interconvert UDP-glcNAc and UDP-galNAc. The strong reduction

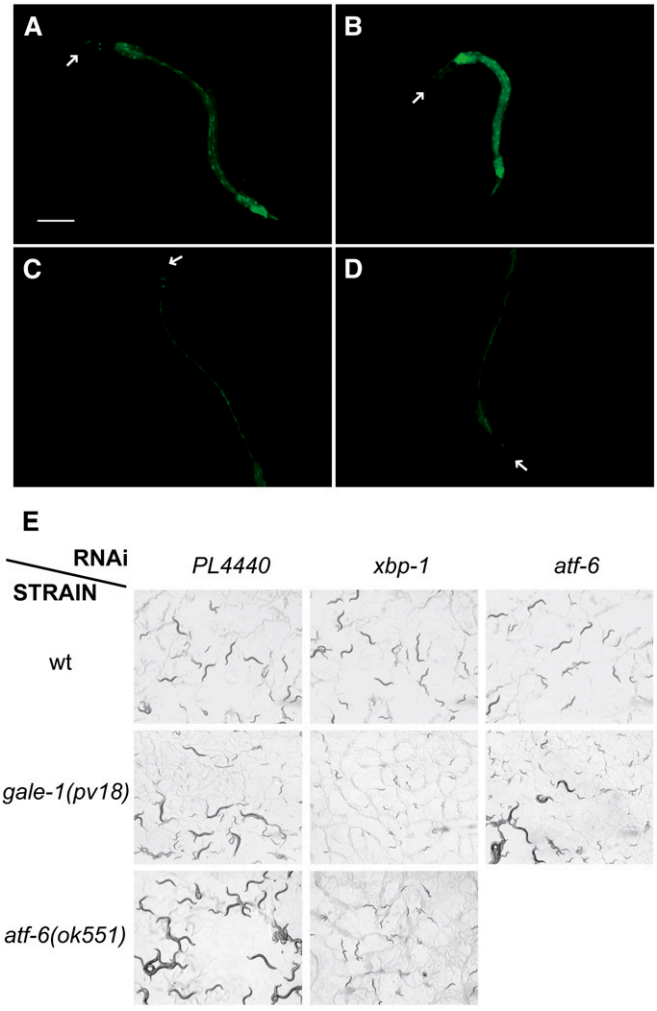

Figure 8 Interaction of *gale-1(pv18)* with the UPR pathway. (A) *hsp-4*::*gfp* expression in a wild-type background. (B) The expression of *hsp-4* is induced in a *gale-1(pv18)* mutant background, indicating that the ER is stressed (see also Figure S4). (C) *hsp-4*::*gfp* expression in animals treated with *xbp-1* RNAi is absent in a wild-type background as well as (D) in a *gale-1(pv18)* mutant background. Arrows indicate the head of the animals. Bar, 100 μm. Animals shown are representative of the population. (E) L4 animals were transferred to RNAi, and the next generation was analyzed. Wild-type animals (top) treated with control pL4440 (empty plasmid), RNAi of *xbp-1*, and *atf-6* reach adulthood. *gale-1(pv18)* (middle) treated with control pL4440 (empty plasmid), RNAi of *xbp-1*, and *atf-6*. Note that *gale-1(pv18)* animals treated with *xbp-1* RNAi arrest at L1 and L2 stages but those treated with *atf-6* RNAi reach adulthood. *atf-6(ok551)* (bottom) treated with control pL4440 (empty plasmid) and RNAi of *xbp-1*. *atf-6(ok551)* similarly to *gale-1(pv18)* animals treated with *xbp-1* RNAi arrested at L2 and L1 stages. *atf-6(ok551)* is in a *fer-15(b26)* background that does not affect this experiment.

of UDP-galNAc observed in the *gale-1(pv18)* mutant indicates that *C. elegans* GALE-1 can accomplish this reaction, similarly to human GALE.

Patients affected by type III galactosemia are sensitive to dietary galactose, likely as a result of the accumulation of toxic intermediary galactose metabolites. As expected, *gale-1(pv18)* animals are hypersensitive to a galactose-rich diet, which has been reported not only for humans but also for *Drosophila* and

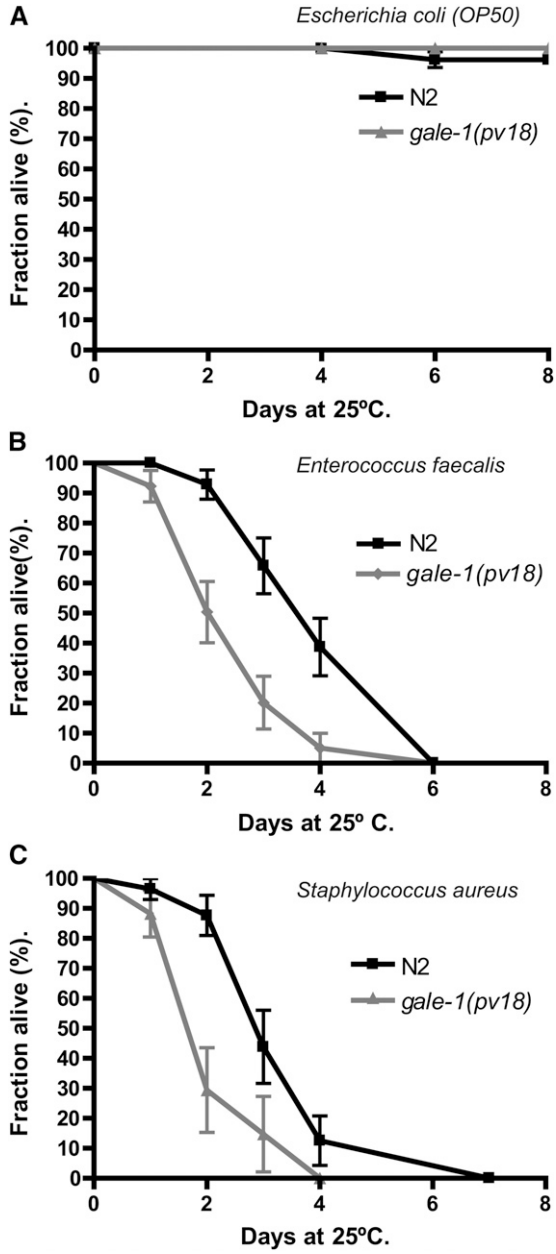

Figure 9 Sensitivity to infection with human bacterial pathogens in *gale-1 (pv18)* mutant and wild-type animals. (A) *gale-1(pv18)* survival in the *E. coli* strain OP50 is not affected. (B) *gale-1(pv18)* is hypersensitive to *E. faecalis*. (C) *gale-1(pv18)* is hypersensitive to *S. aureus*. $n > 30$. Two different trials were assayed with similar results. The Kaplan–Meier statistical analysis was used. In A, no differences between the wild-type and the *gale-1(pv18)* mutant were observed; $P > 0.1$. In B and C, differences between the wild-type and the *gale-1(pv18)* mutant were significant; $P < 0.005$.

Saccharomyces cerevisiae (Walter *et al.* 1999; Ross *et al.* 2004; Sanders *et al.* 2010; McCorvie *et al.* 2011). The toxic effects of elevated galactose concentrations observed in *C. elegans* include developmental delay and arrest in L1 stages. Surprisingly, this effect is produced by adding not only galactose, but also other sugars, although only with galactose is a dose-dependent effect observed, which suggests a more direct interaction with this sugar or with derived metabolites of galactose.

Strikingly, in the wild-type strain, the ER stressor tunicamycin also generates a developmental arrest at or prior to L3 stage (Shen *et al.* 2001), similarly to *ire-1 pek-1*, *atf-6 xbp-1*, or *gale-1 xbp-1* double mutants. Those data suggest that strong ER stress could cause an arrest of development. It is possible that, in the *gale-1(pv18)* mutant, the alteration of the UDP-glucose/galactose rate in a galactose-rich diet and the strong demand of protein folding during development could generate this collapse. Alternatively, accumulation of other metabolites derived specifically from galactose could be responsible for this arrest.

In addition, our analysis strongly suggests that the *gale-1(pv18)* mutant has defects in the glycosylation process; mutant worms exhibit *sqv* and *mig* phenotypes, which are often observed in glycosylation mutants, as well as temperature-sensitive lethality with reduced cellular cohesion. In addition, the MIG-17 metalloprotease, which must be glycosylated to be anchored in the basement membrane, requires GALE-1 for proper localization; although MIG-17 is secreted from the muscle cells in the *gale-1(pv18)* mutant, it fails to accumulate in the gonadal basement membrane. Interestingly, *sqv-7*, which encodes a UDP-glucuronic acid, UDP-gal, and a UDP-GalNAc Golgi transporter, shows a similar phenotype not only in the formation of the vulval lumen (Berninsone *et al.* 2001) but also, as we observed, in gonad migration and MIG-17 localization. These data suggest that the *sqv* and *mig* phenotypes in the *gale-1* and *sqv-7* mutants may result from a decrease in the availability of UDP-galNAc, which is the only sugar defective in both mutants.

UDP-galNAc does not belong to the core branch of N-glycosylation in *C. elegans* and is usually added at the end of the sugar chain (Paschinger *et al.* 2008). Therefore, if MIG-17 is affected by the alteration of UDP-galNAc level, probably the changes in MIG-17 glycosylation will not be profound, but sufficient to impair attachment to the basement membrane of the gonad. Alternatively, the reduction of UDP-galNAc may not affect MIG-17 glycosylation at all. Instead, the alteration of the extracellular matrix, composed of proteoglycans, may impair the migration of MIG-17 from muscle to gonad. In support of this, mutations in the *sqv-5* or in its cofactor *mig-22* genes, which are involved in the formation of chondroitin, also have-gonad migration-defect phenotypes (Suzuki *et al.* 2006).

In this work, we have also observed that a decrease in GALE-1 function activates the unfolded protein response pathway, possibly by generating chronic ER stress. The sugar reduced in *gale-1(pv18)*, UDP-galNAc, does not participate in the glycosylation carried out in the ER (Berninsone 2006), suggesting that the stress observed in this organelle may be caused not by a reduction of this substrate in the ER but by the incorrect glycosylation of proteins involved in ER functions or perhaps by alterations of the UDP-glucose/galactose ratio. Indeed, it has been shown that increased galactose or galactose-derived metabolites induces the activation of the ER stress response by an unknown mechanism in a human cell model of galactosemia (Slepak *et al.* 2005, 2007; Mulhern *et al.* 2006).

gale-1(pv18) animals are hypersensitive to human pathogens. Although we do not know the nature of this sensitivity,

research suggests that ER stress is implicated. This may be due to a possible impairment in secretion of proteins, among them antimicrobial proteins, or to the collapse of ER by the increase of ER stress upon bacterial infection.

Interestingly, hypersensitivity to pathogens has also been described for patients with type I galactosemia (Levy *et al.* 1977; Litchfield and Wells 1978; Waggoner *et al.* 1990; Rathi and Rathi 2011). This phenotype that we observed in the *C. elegans* model for type III galactosemia may be conserved in humans and could have medical implications in the management of patients with type III galactosemia.

In summary, we have characterized two mutations in the gene affected in type III galactosemia, a knockout allele that presents a lethal phenotype and a reduction-of-function allele that is more similar to the mutations found in human patients. The genetic studies using the reduction-of-function allele have generated findings that may have medical implications: hypersensitivity to human pathogens and elevated ER stress. In addition, we observed strong developmental defects in gonad migration and in vulva formation. This model organism and the mutants described here will be useful not only for learning about this disease but also for conducting complementation tests of different human alleles, drug efficacy tests, or large-scale drug screens and thus may be of special interest for designing treatments for type III galactosemia.

Acknowledgments

We thank the Caenorhabditis Genetics Center, Frederick Ausubel, David Baillie, Kijochi Nishiwaki, and the lab of Shohei Mitani through the National Bio-Resource Project of Ministry of Education, Culture, Sports, Science, and Technology, Japan, for providing strains; Peter Askjaer for help with the DeltaVision microscope and critical reading of this manuscript; and Alejandra Cano, Victor Carranco, Valle Rubio, Katherina García, and Ana Isabel López for their excellent technical assistance. The authors declare no competing financial interests. This work was supported by the Junta de Andalucía (P07-CVI-02697) and the Spanish Ministry of Science and Innovation (BFU2006-07391/BMC) and Ministry of Economy and Competitiveness (BFU2013-46923-P). A.M.B.-L. was supported by a Plan Propio de Investigación fellowship from the Universidad Pablo de Olavide. J.M.M. was supported by the Formación del personal Universitario program of the Spanish Ministry of Science and Innovation.

Literature Cited

Bernales, S., F. R. Papa, and P. Walter, 2006 Intracellular signaling by the unfolded protein response. Annu. Rev. Cell Dev. Biol. 22: 487–508.

Berninsone, P. M., 2006 Carbohydrates and glycosylation. (December 18, 2006), WormBook, ed. The C. elegans Research Community, WormBook, doi/10.1895/wormbook.1.125.1, http://www.wormbook.org.

Berninsone, P. M., and C. B. Hirschberg, 2002 The nematode Caenorhabditis elegans as a model to study the roles of proteoglycans. Glycoconj. J. 19: 325–330.

Berninsone, P., H. Y. Hwang, I. Zemtseva, H. R. Horvitz, and C. B. Hirschberg, 2001 SQV-7, a protein involved in Caenorhabditis elegans epithelial invagination and early embryogenesis, transports UDP-glucuronic acid, UDP-N- acetylgalactosamine, and UDP-galactose. Proc. Natl. Acad. Sci. USA 98: 3738–3743.

Brenner, S., 1974 The genetics of *Caenorhabditis elegans*. Genetics 77: 71–94.

Bulik, D. A., and P. W. Robbins, 2002 The Caenorhabditis elegans sqv genes and functions of proteoglycans in development. Biochim. Biophys. Acta 1573: 247–257.

Calfon, M., H. Zeng, F. Urano, J. H. Till, S. R. Hubbard *et al.*, 2002 IRE1 couples endoplasmic reticulum load to secretory capacity by processing the XBP-1 mRNA. Nature 415: 92–96.

Chhay, J. S., C. A. Vargas, T. J. McCorvie, J. L. Fridovich-Keil, and D. J. Timson, 2008 Analysis of UDP-galactose 4′-epimerase mutations associated with the intermediate form of type III galactosaemia. J. Inherit. Metab. Dis. 31: 108–116.

Culetto, E., and D. B. Sattelle, 2000 A role for Caenorhabditis elegans in understanding the function and interactions of human disease genes. Hum. Mol. Genet. 9: 869–877.

Fridovich-Keil, J. L., 2006 Galactosemia: the good, the bad, and the unknown. J. Cell. Physiol. 209: 701–705.

Garsin, D. A., J. M. Villanueva, J. Begun, D. H. Kim, C. D. Sifri *et al.*, 2003 Long-lived C. elegans daf-2 mutants are resistant to bacterial pathogens. Science 300: 1921.

Gems, D., and D. L. Riddle, 2000 Genetic, behavioral and environmental determinants of male longevity in *Caenorhabditis elegans*. Genetics 154: 1597–1610.

Herman, T., E. Hartwieg, and H. R. Horvitz, 1999 sqv mutants of Caenorhabditis elegans are defective in vulval epithelial invagination. Proc. Natl. Acad. Sci. USA 96: 968–973.

Holden, H. M., I. Rayment, and J. B. Thoden, 2003 Structure and function of enzymes of the Leloir pathway for galactose metabolism. J. Biol. Chem. 278: 43885–43888.

Hwang, H. Y., and H. R. Horvitz, 2002 The SQV-1 UDP-glucuronic acid decarboxylase and the SQV-7 nucleotide-sugar transporter may act in the Golgi apparatus to affect Caenorhabditis elegans vulval morphogenesis and embryonic development. Proc. Natl. Acad. Sci. USA 99: 14218–14223.

Hwang, H. Y., S. K. Olson, J. D. Esko, and H. R. Horvitz, 2003 Caenorhabditis elegans early embryogenesis and vulval morphogenesis require chondroitin biosynthesis. Nature 423: 439–443.

Johnston, W. L., A. Krizus, and J. W. Dennis, 2006 The eggshell is required for meiotic fidelity, polar-body extrusion and polarization of the C. elegans embryo. BMC Biol. 4: 35.

Kalckar, H. M., 1965 Galactose metabolism and cell "sociology." Science 150: 305–313.

Kamath, R. S., A. G. Fraser, Y. Dong, G. Poulin, R. Durbin *et al.*, 2003 Systematic functional analysis of the Caenorhabditis elegans genome using RNAi. Nature 421: 231–237.

Kingsley, D. M., K. F. Kozarsky, L. Hobbie, and M. Krieger, 1986 Reversible defects in O-linked glycosylation and LDL receptor expression in a UDP-Gal/UDP-GalNAc 4-epimerase deficient mutant. Cell 44: 749–759.

Krieger, M., P. Reddy, K. Kozarsky, D. Kingsley, L. Hobbie *et al.*, 1989 Analysis of the synthesis, intracellular sorting, and function of glycoproteins using a mammalian cell mutant with reversible glycosylation defects. Methods Cell Biol. 32: 57–84.

Kubota, Y., and K. Nishiwaki, 2006 C. elegans as a model system to study the function of the COG complex in animal development. Biol. Chem. 387: 1031–1035.

Kubota, Y., M. Sano, S. Goda, N. Suzuki, and K. Nishiwaki, 2006 The conserved oligomeric Golgi complex acts in organ

morphogenesis via glycosylation of an ADAM protease in C. elegans. Development 133: 263–273.
Kuwabara, P. E., and N. O'Neil, 2001 The use of functional genomics in C. elegans for studying human development and disease. J. Inherit. Metab. Dis. 24: 127–138.
Lee, A. S., 1992 Mammalian stress response: induction of the glucose-regulated protein family. Curr. Opin. Cell Biol. 4: 267–273.
Levy, H. L., S. J. Sepe, V. E. Shih, G. F. Vawter, and J. O. Klein, 1977 Sepsis due to Escherichia coli in neonates with galactosemia. N. Engl. J. Med. 297: 823–825.
Litchfield, W. J., and W. W. Wells, 1978 Effect of galactose on free radical reactions of polymorphonuclear leukocytes. Arch. Biochem. Biophys. 188: 26–30.
Maley, F., and G. F. Maley, 1959 The enzymic conversion of glucosamine to galactosamine. Biochim. Biophys. Acta 31: 577–578.
Malhotra, J. D., and R. J. Kaufman, 2007 The endoplasmic reticulum and the unfolded protein response. Semin. Cell Dev. Biol. 18: 716–731.
McCorvie, T. J., J. Wasilenko, Y. Liu, J. L. Fridovich-Keil, and D. J. Timson, 2011 In vivo and in vitro function of human UDP-galactose 4′-epimerase variants. Biochimie 93: 1747–1754.
Mulhern, M. L., C. J. Madson, A. Danford, K. Ikesugi, P. F. Kador *et al.*, 2006 The unfolded protein response in lens epithelial cells from galactosemic rat lenses. Invest. Ophthalmol. Vis. Sci. 47: 3951–3959.
Munoz, M. J., and D. L. Riddle, 2003 Positive selection of *Caenorhabditis elegans* mutants with increased stress resistance and longevity. Genetics 163: 171–180.
Nishiwaki, K., N. Hisamoto, and K. Matsumoto, 2000 A metalloprotease disintegrin that controls cell migration in Caenorhabditis elegans. Science 288: 2205–2208.
Nishiwaki, K., Y. Kubota, Y. Chigira, S. K. Roy, M. Suzuki *et al.*, 2004 An NDPase links ADAM protease glycosylation with organ morphogenesis in C. elegans. Nat. Cell Biol. 6: 31–37.
Paschinger, K., M. Gutternigg, D. Rendic, and I. B. Wilson, 2008 The N-glycosylation pattern of Caenorhabditis elegans. Carbohydr. Res. 343: 2041–2049.
Piller, F., M. H. Hanlon, and R. L. Hill, 1983 Co-purification and characterization of UDP-glucose 4-epimerase and UDP-N-acetylglucosamine 4-epimerase from porcine submaxillary glands. J. Biol. Chem. 258: 10774–10778.
Quimby, B. B., A. Alano, S. Almashanu, A. M. DeSandro, T. M. Cowan *et al.*, 1997 Characterization of two mutations associated with epimerase-deficiency galactosemia, by use of a yeast expression system for human UDP-galactose-4-epimerase. Am. J. Hum. Genet. 61: 590–598.
Rathi, N., and A. Rathi, 2011 Galactosemia presenting as recurrent sepsis. J. Trop. Pediatr. 57: 487–489.
Ross, K. L., C. N. Davis, and J. L. Fridovich-Keil, 2004 Differential roles of the Leloir pathway enzymes and metabolites in defining galactose sensitivity in yeast. Mol. Genet. Metab. 83: 103–116.
Sanders, R. D., J. M. Sefton, K. H. Moberg, and J. L. Fridovich-Keil, 2010 UDP-galactose 4′ epimerase (GALE) is essential for development of Drosophila melanogaster. Dis. Model. Mech. 3: 628–638.
Schachter, H., 2004 Protein glycosylation lessons from Caenorhabditis elegans. Curr. Opin. Struct. Biol. 14: 607–616.
Schroder, M., and R. J. Kaufman, 2005a ER stress and the unfolded protein response. Mutat. Res. 569: 29–63.
Schroder, M., and R. J. Kaufman, 2005b The mammalian unfolded protein response. Annu. Rev. Biochem. 74: 739–789.
Schulz, J. M., A. L. Watson, R. Sanders, K. L. Ross, J. B. Thoden *et al.*, 2004 Determinants of function and substrate specificity in human UDP-galactose 4′-epimerase. J. Biol. Chem. 279: 32796–32803.
Schulz, J. M., K. L. Ross, K. Malmstrom, M. Krieger, and J. L. Fridovich-Keil, 2005 Mediators of galactose sensitivity in UDP-galactose 4′-epimerase-impaired mammalian cells. J. Biol. Chem. 280: 13493–13502.
Shen, X., R. E. Ellis, K. Lee, C. Y. Liu, K. Yang *et al.*, 2001 Complementary signaling pathways regulate the unfolded protein response and are required for C. elegans development. Cell 107: 893–903.
Shen, X., R. E. Ellis, K. Sakaki, and R. J. Kaufman, 2005 Genetic interactions due to constitutive and inducible gene regulation mediated by the unfolded protein response in C. elegans. PLoS Genet. 1: e37.
Sifri, C. D., J. Begun, and F. M. Ausubel, 2005 The worm has turned: microbial virulence modeled in Caenorhabditis elegans. Trends Microbiol. 13: 119–127.
Slepak, T., M. Tang, F. Addo, and K. Lai, 2005 Intracellular galactose-1-phosphate accumulation leads to environmental stress response in yeast model. Mol. Genet. Metab. 86: 360–371.
Slepak, T. I., M. Tang, V. Z. Slepak, and K. Lai, 2007 Involvement of endoplasmic reticulum stress in a novel classic galactosemia model. Mol. Genet. Metab. 92: 78–87.
Suzuki, N., H. Toyoda, M. Sano, and K. Nishiwaki, 2006 Chondroitin acts in the guidance of gonadal distal tip cells in C. elegans. Dev. Biol. 300: 635–646.
Thoden, J. B., and H. M. Holden, 1998 Dramatic differences in the binding of UDP-galactose and UDP-glucose to UDP-galactose 4-epimerase from Escherichia coli. Biochemistry 37: 11469–11477.
Thoden, J. B., T. M. Wohlers, J. L. Fridovich-Keil, and H. M. Holden, 2001 Human UDP-galactose 4-epimerase. Accommodation of UDP-N-acetylglucosamine within the active site. J. Biol. Chem. 276: 15131–15136.
Thoden, J. B., J. M. Henderson, J. L. Fridovich-Keil, and H. M. Holden, 2002 Structural analysis of the Y299C mutant of Escherichia coli UDP-galactose 4-epimerase. Teaching an old dog new tricks. J. Biol. Chem. 277: 27528–27534.
Timson, D. J., 2006 The structural and molecular biology of type III galactosemia. IUBMB Life 58: 83–89.
Tirasophon, W., A. A. Welihinda, and R. J. Kaufman, 1998 A stress response pathway from the endoplasmic reticulum to the nucleus requires a novel bifunctional protein kinase/endoribonuclease (Ire1p) in mammalian cells. Genes Dev. 12: 1812–1824.
Waggoner, D. D., N. R. Buist, and G. N. Donnell, 1990 Long-term prognosis in galactosaemia: results of a survey of 350 cases. J. Inherit. Metab. Dis. 13: 802–818.
Walter, J. H., R. E. Roberts, G. T. Besley, J. E. Wraith, M. A. Cleary *et al.*, 1999 Generalised uridine diphosphate galactose-4-epimerase deficiency. Arch. Dis. Child. 80: 374–376.
Wang, X. Z., H. P. Harding, Y. Zhang, E. M. Jolicoeur, M. Kuroda *et al.*, 1998 Cloning of mammalian Ire1 reveals diversity in the ER stress responses. EMBO J. 17: 5708–5717.
Wasilenko, J., M. E. Lucas, J. B. Thoden, H. M. Holden, and J. L. Fridovich-Keil, 2005 Functional characterization of the K257R and G319E-hGALE alleles found in patients with ostensibly peripheral epimerase deficiency galactosemia. Mol. Genet. Metab. 84: 32–38.
Wicks, S. R., R. T. Yeh, W. R. Gish, R. H. Waterston, and R. H. Plasterk, 2001 Rapid gene mapping in Caenorhabditis elegans using a high density polymorphism map. Nat. Genet. 28: 160–164.
Wilm, T., P. Demel, H. U. Koop, H. Schnabel, and R. Schnabel, 1999 Ballistic transformation of Caenorhabditis elegans. Gene 229: 31–35.
Wohlers, T. M., N. C. Christacos, M. T. Harreman, and J. L. Fridovich-Keil, 1999 Identification and characterization of a mutation, in the human UDP-galactose-4-epimerase gene, associated with generalized epimerase-deficiency galactosemia. Am. J. Hum. Genet. 64: 462–470.
Zwaal, R. R., K. Van Baelen, J. T. Groenen, A. van Geel, V. Rottiers *et al.*, 2001 The sarco-endoplasmic reticulum Ca2+ ATPase is required for development and muscle function in Caenorhabditis elegans. J. Biol. Chem. 276: 43557–43563.

Communicating editor: M. V. Sundaram

GENETICS

Supporting Information
http://www.genetics.org/lookup/suppl/doi:10.1534/genetics.114.170084/-/DC1

Developmental Defects in a *Caenorhabditis elegans* Model for Type III Galactosemia

Ana M. Brokate-Llanos, José M. Monje, Piedad del Socorro Murdoch, and Manuel J. Muñoz

DOI: 10.1534/genetics.114.170084

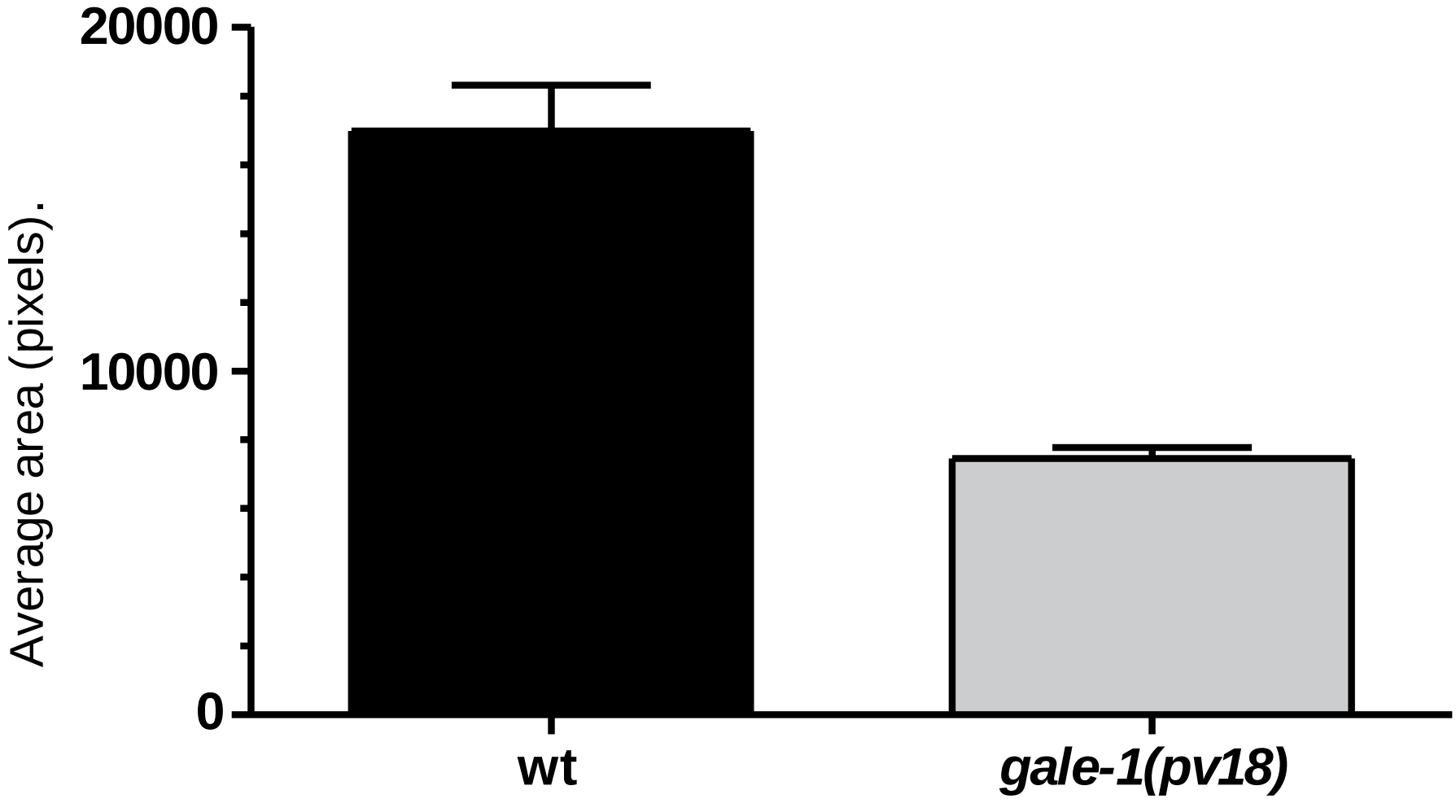

Figure S1: The size of the vulva of *gale-1(pv18)* is reduced: The area of the vulva has been measure by counting the total pixel that occupies in the photography. *gale-1(pv18)* showed half of the size of a wild type vulva. N=20. P > 0.0001

The area was meassure with the ImageJ software and for the statistic test we used Graphpad Prism.

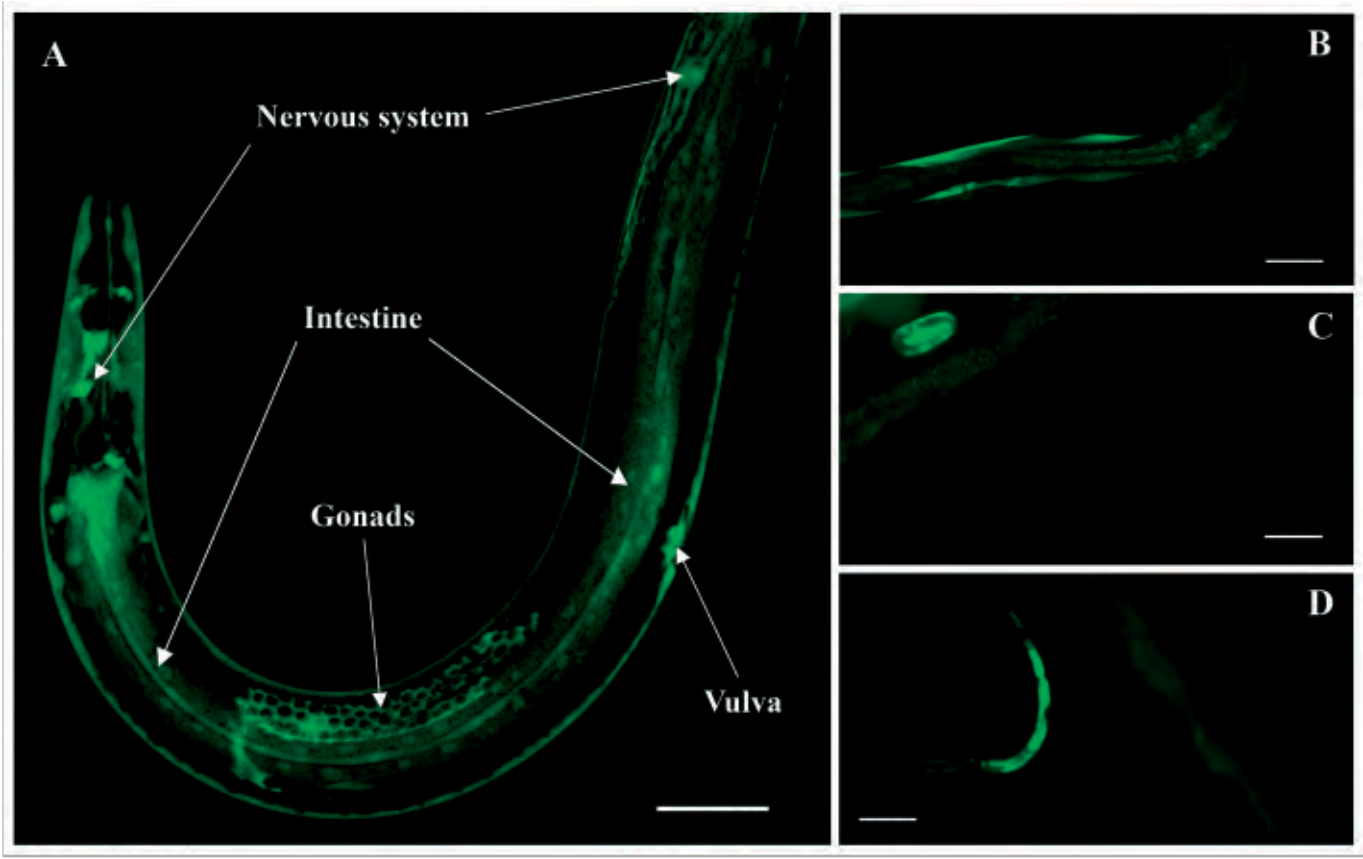

Figure S2: Expression of GFP under the *gale-1* promoter. (A) Expression is observed in gonads, vulva, intestine, hypodermis and nervous system. (B) As also in muscle cells. This late tissue is relevant because is where MIG-17 is produced and secreted to reach gonad basement membrane. (C) The expression is higher in embryos and (D) L1 stage. Images for figure A were captured using a TCS SP2 confocal microscope equipped with an HCX PL APO 40×/1.25 objective lens. Images were taken using integrated Leica software and processed with ImageJ and Adobe Photoshop. Figures B, C and D were acquired as described in material and methods for SJ4005 and GM266 strains.

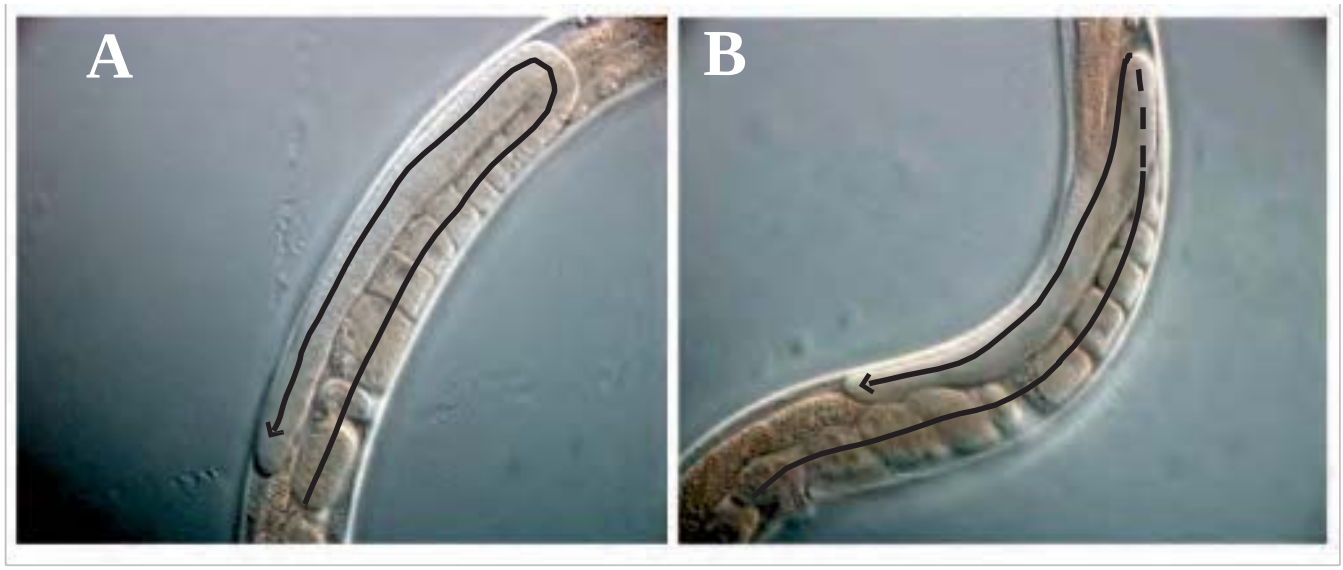

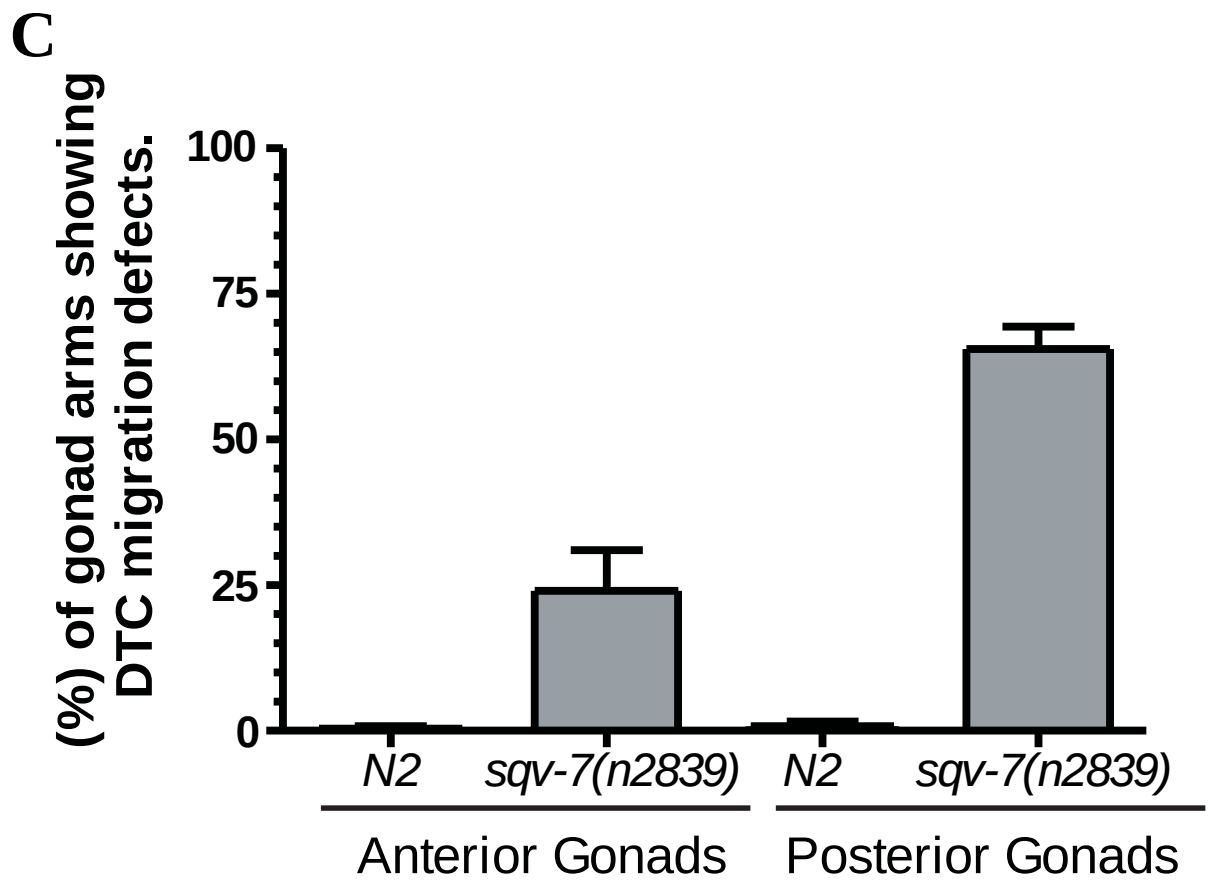

Figure S3: *sqv-7(n2839)* has gonad migration defects: (A) Gonad of a wild type animal. (B) Gonad of a *sqv-7(n2839)* mutant. The gonad in this mutant does not have the characteristic U-shape, similarly to the *gale-1(pv18)* mutant. (C) Percentage of anterior and posterior gonads affected. N>20. $P < 0.05$

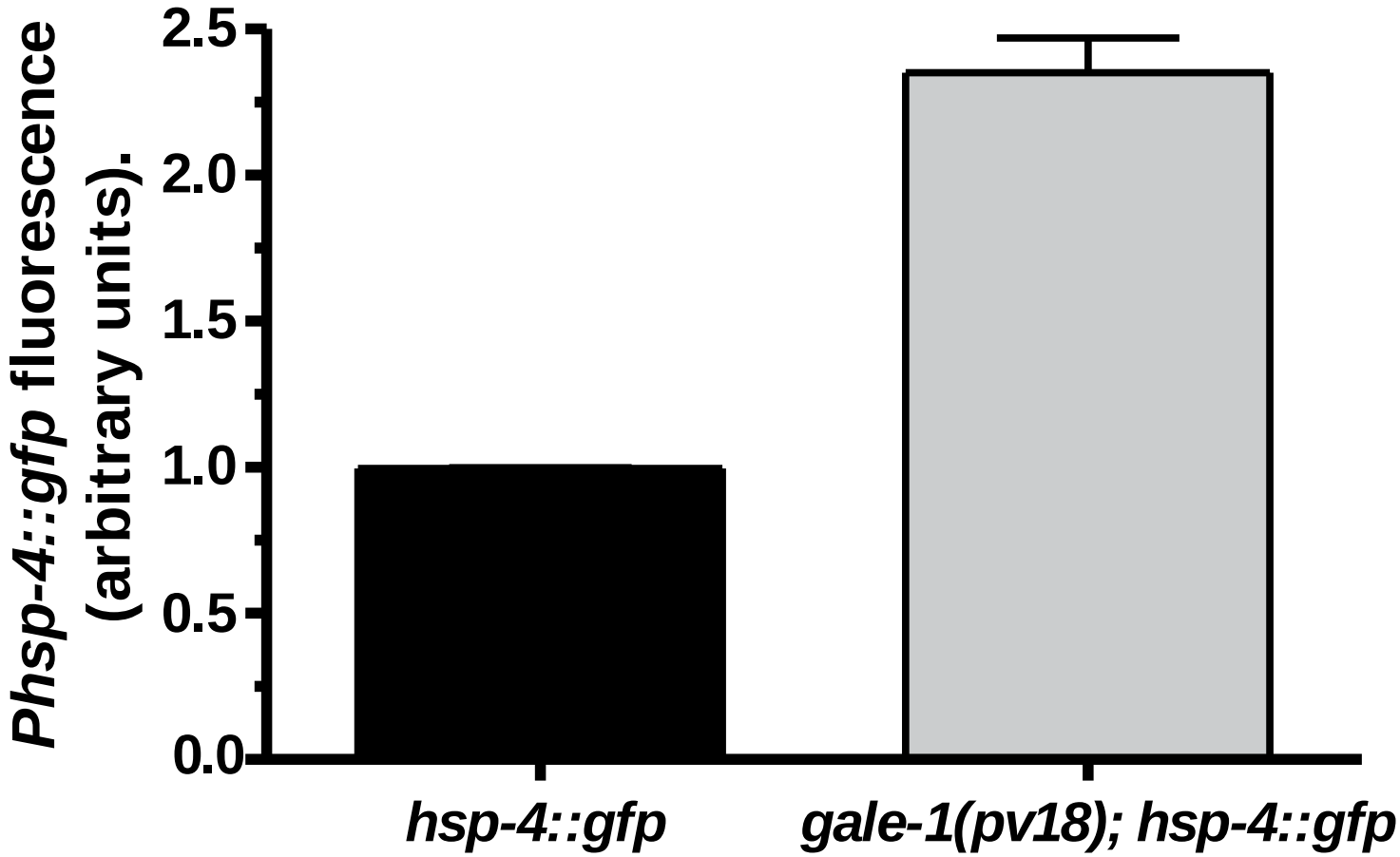

Figure S4: *hsp-4* expression in *gale-1(pv18)* mutant background. Quantification of the expression of *hsp-4* in a wild type and in *gale-1(pv18)* mutant. The fluorescence levels were relative to the mean of *hsp-4::gfp* in a wild type background. For quantification, we analysed 1388 × 1040 pixel 16-bit greyscale images using ImageJ with the MacBiophotonics plugins. For each individual trial, exposure time was calibrated to avoid saturated pixels for the set of animals. N>76. P > 0.005

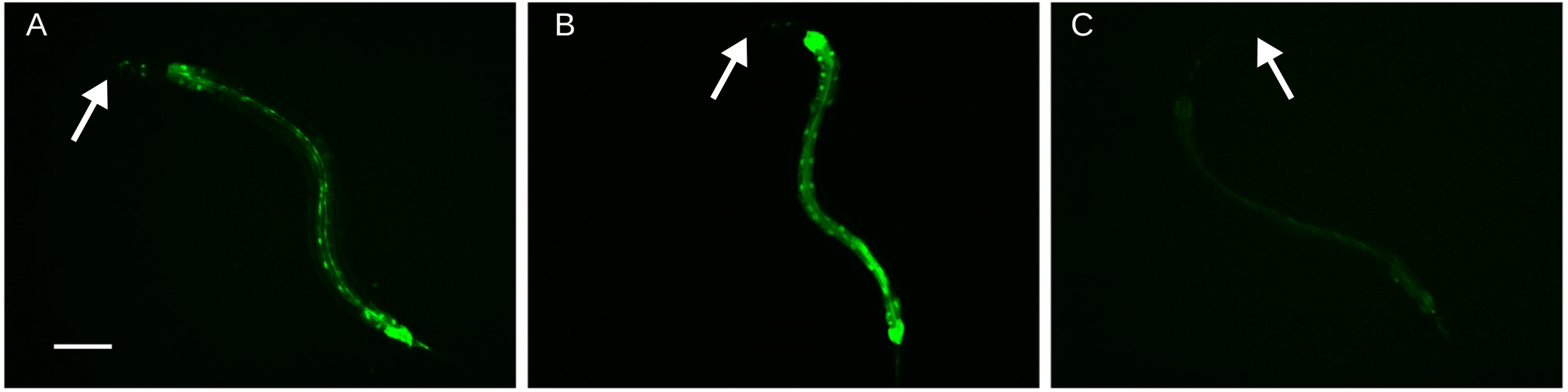

Figure S5: Interaction of *atf-6(ok551)* with the UPR pathway. (A) *hsp-4::gfp* expression in a wild-type background (same as figure 8A). (B) The expression of *hsp-4* is induced in a *atf-6(ok551)* mutant background, indicating that the ER is stressed. (C) *hsp-4::gfp* expression in animals treated with *xbp-1* RNAi is absent in a *atf-6(ok551)* mutant background. Arrows indicate the head of the animals. The scale bar represents 100 µm. Animals shown are representative of the population.

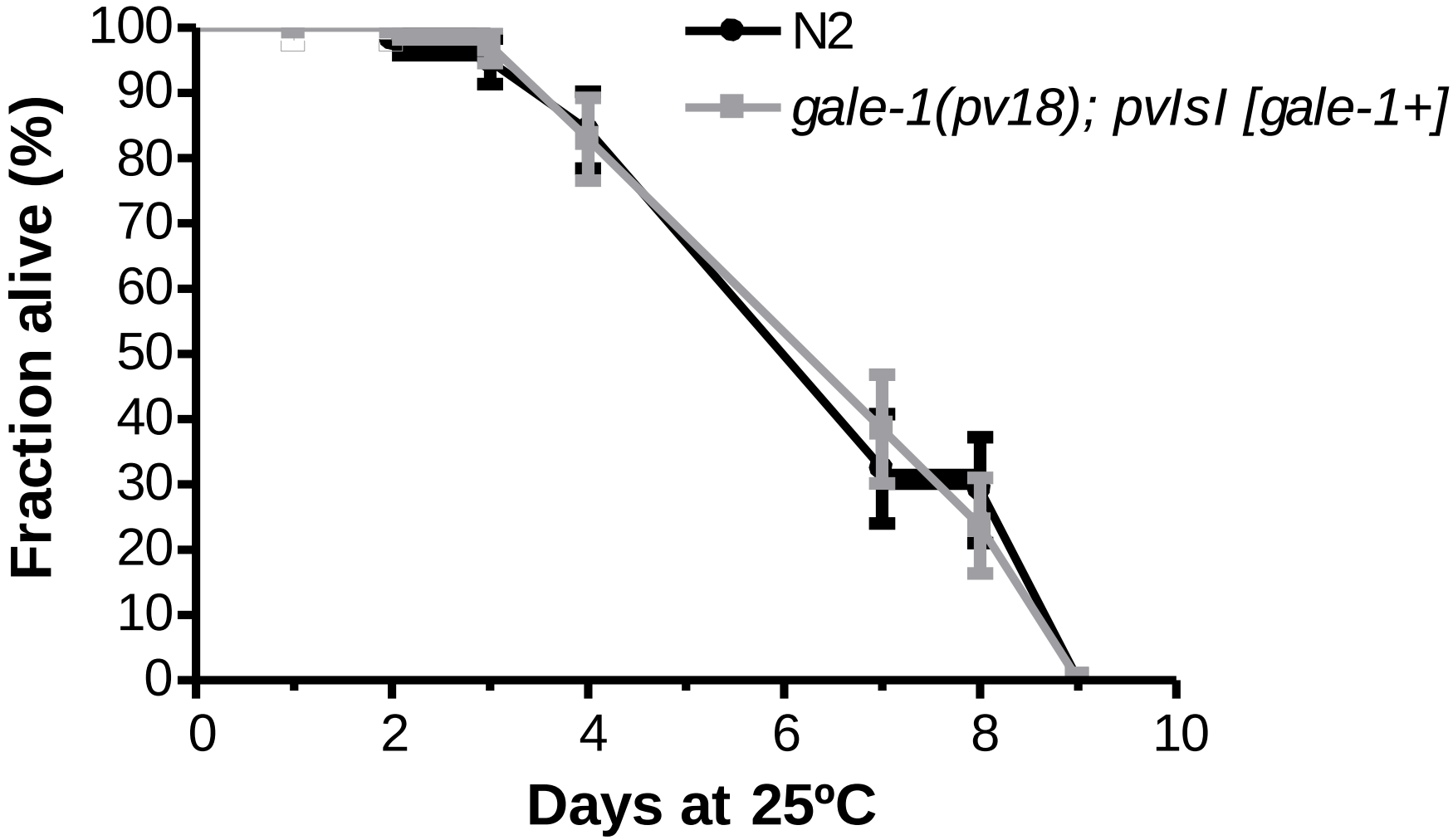

Figure S6: Survival of *gale-1(pv18)* carrying a construction of *gale-1+* in the presence of *Enterococcus faecalis*. No differences are observed with the wild-type strain (P>0.5), indicating that the expression of the *gale-1+* rescues the hypersensivity to infection.

Table S1: Developmental delay of the *gale-1(pv18)* mutant: Wild type *C. elegans* develop from the first larval stage L1 to L4 and then to adult in 3 days either at 16ºC or 20ºC. However *gale-1(pv18)* needs up to 5 days to reach adulthood. * Those strains are in a *fer-15(b26)* background, this mutation affects sperm production at 25ºC but does not affect development. N>200.

Strain	Days	16ºC	20ºC
*Wild type**	3 Days	90±6% Young adult	100% Adult
*gale-1(pv18)**	3 Days	100% L2 or L3	64±9% L1
	5 Days	82±6% Young adult	67±7% Young adult

File S1: Embryonic development of *gale-1(pv18)* mutant is impaired: At 25ºC, wild type embryos hatch after normal development (top embryo); however most of the *gale-1(pv18)* animals do not hatch (the two bottom embryos). Instead, we can observe that during development cells do not tie together may be due to defect in cell adhesion or fail in the hypodermal enclose.

Observation of embryogenesis was performed on an Applied Precision DeltaVision microscope system enclosed in a temperature-controlled chamber set at 25°C. Embryos from wild type and *gale-1 (pv18)* animals were mounted together in M9 buffer on a 3% agarose pad and coverslips were sealed with Valap to avoid desiccation. Images were acquired every minute for a total of 16 hours.

Available for download as a .mov file at
http://www.genetics.org/lookup/suppl/doi:10.1534/genetics.114.170084/-/DC1